



Study of the Solidification Behavior and Porosity Measurements to Enhance Fatigue Life of HPDC Aluminum Swing Arm Design

Dinesh Dhande · Nitin Choudhari

Submitted: 6 December 2023 / in revised form: 15 August 2024 / Accepted: 16 August 2024
© ASM International 2024

Abstract In light of fuel consumption reduction and environmental regulations, the automotive industry favors lightweight components. Aluminum is chosen for its superior corrosion resistance and high strength-to-weight ratio in complex vehicle parts which are manufactured using high pressure die-casting (HPDC) process. However, this process suffers from significant mechanical property variations and unreliable stress cycles due to defects like porosity, shrinkage, misrun, and hot tears, leading to fatigue failures. Despite the detrimental impact of casting defects, the underlying reasons for the high variability in the HPDC process remain unclear. Numerical tools provide insights into parameters that are challenging to measure experimentally. This research presents a thorough analysis of the design, development, fabrication, and testing of an aluminum die-cast swing arm utilizing Magma 5 software. The study focuses on the solidification characteristics of the swing arm, examining factors such as pore length, solidification duration, hot spot distribution, and shrinkage porosity severity. To support design improvements aimed at addressing identified failures, the commercial simulation software Magma 5 was employed. These enhancements resulted in a substantial reduction in solidification time and effectively shifted hot spots away from previously identified cracked areas. Additionally, there were significant

decreases in both the percentage and intensity of porosity, confirmed by X-ray and CT scan analyses. Durability tests conducted with a dynamometer indicated a remarkable 50% increase in fatigue life compared to the original design. The research highlights the significance of early simulation-based design modifications in reducing fatigue failures in HPDC aluminum components. It was noted that excessive porosity levels exceeding 8% are a major factor contributing to this issue. Recommendations include avoiding thicker designs and complex part configurations to reduce porosity, as well as assessing defect locations in relation to surface proximity and stress regions.

Keywords Aluminum casting defects · Cast flow analysis · Fatigue failure · Solidification behavior · Porosity

Introduction

Aluminum castings are increasingly preferred in the automotive industry due to their lightweight characteristics and low density, meeting the growing demand for internal combustion engine (ICE) and electric vehicles (EVs) with extended ranges. This shift toward aluminum for structural components, such as frames and wheels, is driven by the need to reduce vehicle weight. Benefits of aluminum castings include the ability to create complex shapes cost-effectively, excellent machining performance and thermal conductivity, and a high strength-to-weight ratio [1]. However, challenges such as inevitable casting defects and uncertainties in mechanical properties may limit their application in high-performance structural components [2–6, 8, 16] and needs to be studied in depth.

D. Dhande (✉) · N. Choudhari
Department of Mechanical Engineering, AISSMS College of
Engineering, Pune 411001, India
e-mail: dydhande@aissmscoe.com

N. Choudhari
Hero MotoCorp Ltd., Jaipur 302028, India
e-mail: nitin.choudhari@heromotocorp.com

The researchers have focused on reducing porosity in castings to enhance their structural integrity and performance. Fatigue loading often causes cracks to initiate and grow at porosity defects in cast components. Significant differences between predicted and actual fatigue life have been noted, largely due to the complexities of real casting processes that yield various flaw types [3]. To establish a reliable correlation between theoretical and actual fatigue life, fatigue analyses on actual components must be conducted and compared to theoretical results. Experimental research has provided valuable insights into the relationship between pore characteristics and fatigue life. Casting simulations indicate that reducing porosity, optimizing its distribution, and minimizing pore sizes can greatly improve fatigue resistance. Additionally, studies have employed commercial simulation software to forecast the distribution of shrinkage defects in castings, highlighting the critical impact of mold preheating temperature on casting quality [4].

Despite significant progress, the precise influence of porosity on component performance remains unclear. While strategies to reduce porosity have been established, empirical assessments of their impact are still lacking [5]. Advancements in computational simulations have improved understanding of solidification phenomena in casting processes, allowing for the analysis of complex physical processes and difficult-to-measure quantities [6]. Nevertheless, accurately predicting casting performance continues to face challenges, particularly with defects like cracks and porosity. Research highlights a critical pouring temperature threshold, beyond which increased temperatures may raise porosity levels, while higher pouring rates can mitigate it [7]. Characterizing fatigue properties in large structures necessitates accounting for variables like stress concentration, scale, and process parameters. Stress concentration at geometric imperfections is the primary contributor to fatigue damage. Additionally, fatigue characteristics are affected by structural size, internal flaws, and the manufacturing process employed [8]. Effective optimization techniques, including adjustments to pouring temperatures and gating configurations, have proven successful in reducing porosity, emphasizing the need for a synergy between simulation and physical testing in casting processes [9].

Comparative studies of vacuum die casting versus traditional high-pressure die casting (HPDC) reveal significant reductions in porosity, confirmed through X-ray and SEM assessments [10]. The use of simulation software has become essential for optimizing casting processes, enhancing quality, and mitigating defects [11], while also highlighting the critical need to validate simulations with physical prototypes [12, 13]. Moreover, research into squeeze casting indicates its potential for producing high-

quality castings, although challenges such as residual stresses in thin-walled geometries and persistent porosity issues remain, particularly influenced by cooling rates and casting designs [14, 15].

The mechanical performance of cast components is greatly affected by porosity. Low-porosity plates tend to crack at surface flaws known as externally solidified crystals (ESCs) due to poor bonding. Conversely, in highly porous plates, cracks propagate through pore enlargement and the failure of smaller interconnected pores, highlighting porosity's critical role in mechanical properties and elongation [17].

Crucial parameters for casting quality include critical defect sizes and secondary dendrite spacing. Studies have established relationships between maximum fracture stress and porosity, with stress intensity factors influenced by pore characteristics. Eutectic silicon bands and Fe-rich phases significantly affect crack resistance and propagation, while increased silicone and copper levels can shorten component fatigue life [18–20]. Research indicates that high porosity negatively impacts mechanical properties, but small, uniformly distributed pores are less detrimental compared to larger, scattered ones. Critical thresholds for porosity and pore size are vital in determining mechanical properties [21]. Investigations into microstructure evolution and fracture mechanisms under quasi-static uniaxial loading show microcracks can initiate at the silicon–aluminum matrix interfaces, leading to structural fracture [22]. A systematic framework for analyzing structure fatigue reliability has been introduced to comprehensively evaluate the fatigue life of cast components. Casting defects, such as porosity and uneven microstructure, significantly challenge the durability and performance of cast components, making it essential to understand their impact on fatigue life. The transfer coupling data method, utilizing software to predict fatigue behavior, has proven effective for these issues [23]. Initially, ProCAST was employed for cast flow analysis to predict shrinkage cavities and microdefects, which were then mapped onto an Abacus model for controlled analysis of wheel fatigue behavior. Ultimately, defect data was transferred to the FESafe model for fatigue life analysis under specific conditions, greatly reducing error rates through enhanced simulation techniques [24].

The influence of critical defect size on danger coefficients indicates that smaller defects predict greater structural strength [25]. The Taguchi DoE method is effective for optimizing casting parameters [26]. Research shows tensile strength decreases with increased porosity, while fatigue strength remains stable across porosity variations. Pore size and location are significant in fatigue strength assessment, with less stressed pores having minimal effects [27]. Mechanical property studies indicate that die-casting processes outperform other manufacturing

methods for aluminum alloys [28]. Model-based predictive control solutions have been developed to improve low-pressure die-casting performance for aluminum wheels [29]. The correlation between heat treatment and casting defect evolution has been extensively researched. Cold flakes from crystallization in gating systems lead to blistering, reducing ductility [30]. Optimal squeezing pressure enhances aluminum alloy tensile strength, yield strength, hardness, and elongation significantly, while reducing shrinkage porosity [31].

Porosity is the primary cause of casting part rejection. Simulation can predict and mitigate porosity through effective casting software use [32]. Simulation technology can enhance cooling and insulation processes, preventing premature feeding path cutoffs and reducing hot spot sizes. Porosity contours from simulations were compared with actual X-ray inspections to establish correlations [33]. Employing a vacuum in the die cavity enhances yield strength by 8.4% relative to non-vacuum scenarios. The mechanical properties of A380 aluminum alloy improve with rising injection pressure, with a 15% increase in yield strength noted when pressure escalates from 100 to 200 bar. The use of vacuum casting correlates with reduced porosity levels [34]. The smoothed particle hydrodynamics (SPH) method demonstrates proficiency in predicting die cavity filling quality. It offers the die-casting sector enhanced predictive capabilities for the HPDC process, resulting in thinner, lighter parts, improved cycle times, reduced scrap, and expedited die development [35]. Specific temperature gradients established within the die contribute to superior casting quality and reduced cycle times, ultimately extending die service life [36]. The process parameters were optimized to achieve minimal porosity in high-pressure die aluminum casting. An 85% accurate porosity predictive model was created for finished casting parts [37]. Elevated melt temperatures (785 and 850 °C) positively influenced primary Si crystal size and distribution, although excessively high temperatures may be impractical [38].

Casting defects adversely affect aluminum die-cast components' functionality and reliability. Establishing a consistent correlation between simulation results and actual tests is still problematic. Current research lacks quantitative assessments of porosity and its impact on fatigue strength. Although the negative impact of casting defects on fatigue life is recognized, viable solutions are scarce. This study highlights the necessity for thorough investigations aimed at reducing casting porosity and enhancing fatigue life. It suggests conducting experiments or simulations to optimize the relationship between porosity and fatigue life. A comprehensive analysis will include variables such as design, simulations, X-rays, CT scans, adjustments, and fatigue testing. Root-cause analysis

techniques are essential for resolving issues related to porosity and shrinkage in casting failures. An in-depth examination of a high-pressure die-casting aluminum swing arm offers insights into porosity beyond mechanical responses. The findings recommend methods to improve design and development to mitigate porosity and enhance fatigue life. Evaluating solidification behavior during design through cast flow analysis aids in boosting component reliability. This research emphasizes the intricate nature of failure analysis and the critical need for extensive testing, simulation, and evaluation to ensure the reliability of essential vehicle components.

Materials and Methods

The swing arm in an internal combustion engine of the scooter is essential for wheel integrity, force transfer, structural load endurance, and muffler mounting. Its critical role in vehicle dynamics and rider safety warrants analysis due to its exposure to road shocks and reported fatigue failures.

Experimental Investigation

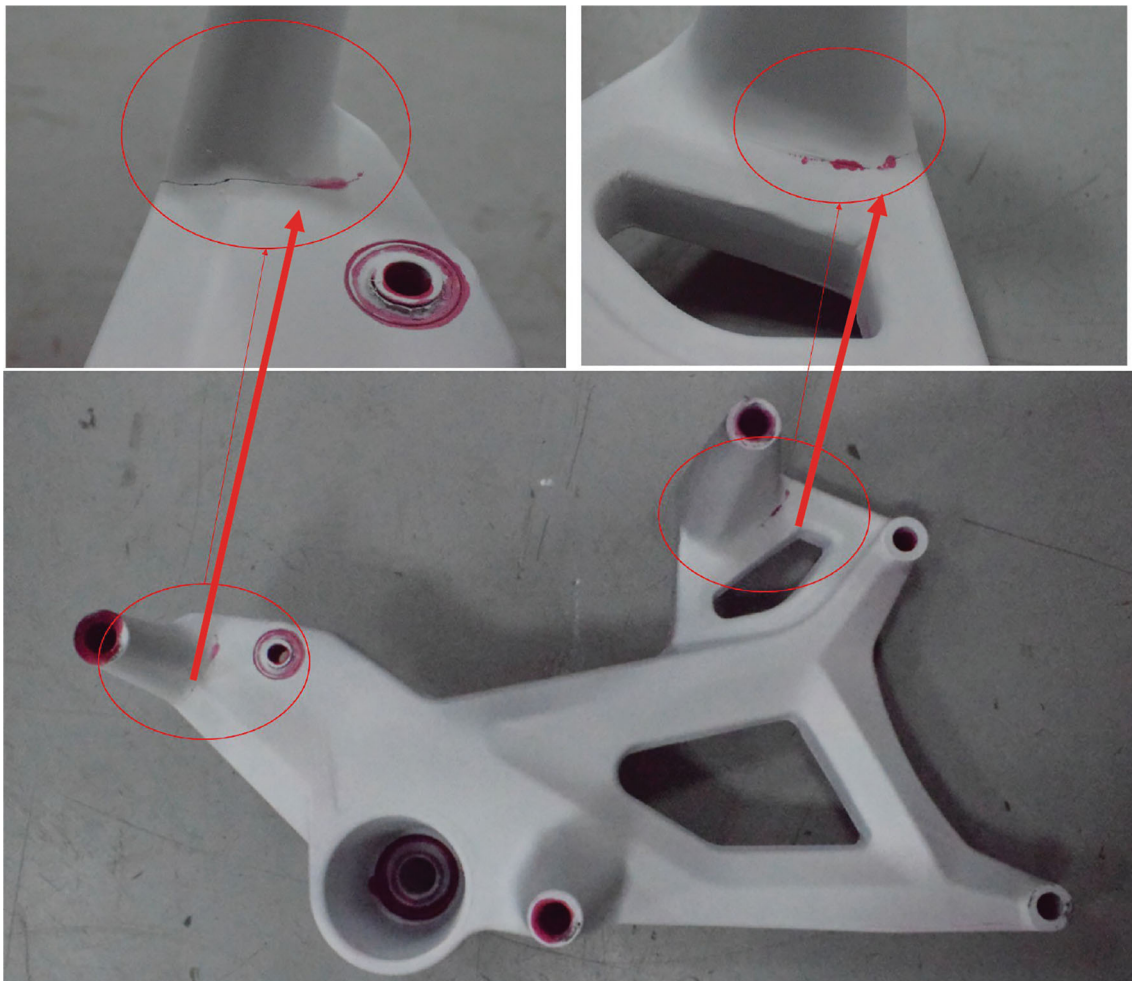
The experimental study involved road endurance testing of the scooter at 24 °C and 50% humidity, with one test cycle lasting approximately 1 min. Each cycle included accelerating to 100 km/h, maintaining speed for thirty seconds, and then de-throttling. A hairline crack was detected in the swing arm assembly after 66.6 h (4000 cycles) of testing, equivalent to 12,000 km of usage, despite the design having a safety factor exceeding 1.5 in simulations. This prompted a comprehensive re-evaluation of engineering aspects, although no significant design flaws were initially found.

The failed component underwent inspection to ensure drawing compliance, with satisfactory results from dimensional checks using a coordinate measuring machine (CMM). Material and morphology analysis done using X-ray spectroscopy and scanning electron microscope, respectively, confirmed the use of AlSi11Cu3 (ADC 12) alloy, and no abnormalities were discovered during the investigation of assembly and impact marks. The chemical composition of the failed part was also analyzed and is listed in Table 1.

An extensive 8D analysis was conducted to identify the root cause of the failure, leading to corrective actions. Structural stiffness and strength were confirmed to be within acceptable limits, as previously validated by finite element analysis (FEA) and actual testing, ruling them out as failure causes. Additionally, all potential failure modes were addressed through a risk mitigation strategy during

Table 1 Chemical composition of failed swing arm

Material	Elements (%)											
	Cu	Si	Mg	Fe	Sn	Zn	Pb	Cr	Ti	Ni	Mn	
ADC 12 AS per JIS H 5302												
Specification	1.5–3.5	9.6–12	0.3 Max	1.3 Max	0.2 Max	1.0 Max	0.1 Max	...	0.3 Max	0.5 Max	0.5 Max	
Measured (X-ray spectroscopy)	1.94	10.46	0.09	0.96	0.02	1.42	0.119	0.02	0.04	0.11	0.18	

**Fig. 1** Failed swing arm

the design and development phases. The failure of the HPDC aluminum swing arm during road endurance durability testing in a fleet vehicle at 66.6 h is depicted in Fig. 1.

During the 8D analysis, a focus was placed on the manufacturing process of the component, revealing that the high-pressure die-casting (HPDC) method for the swing arm part is prone to porosity. An examination of the failed HPDC aluminum swing arm indicated a significant porosity cluster near the crack initiation point as depicted in Fig. 2, supporting the hypothesis that casting defects were responsible for the failure.

A decision was made to utilize Magma 5 simulation software to evaluate solidification behavior and identify potential porosity regions in a virtual model. Concurrently, X-ray and CT scans were performed on actual components from the same production batch to detect porosity.

Numerical Analysis

Solidification Behavior Simulation to Simulate the Porosity The 3D model of the defective HPDC aluminum swing arm was analyzed within Magma 5 to simulate porosity based on the failed part, focusing on parameters to



Fig. 2 Failed part cut-section images to check the porosity regions

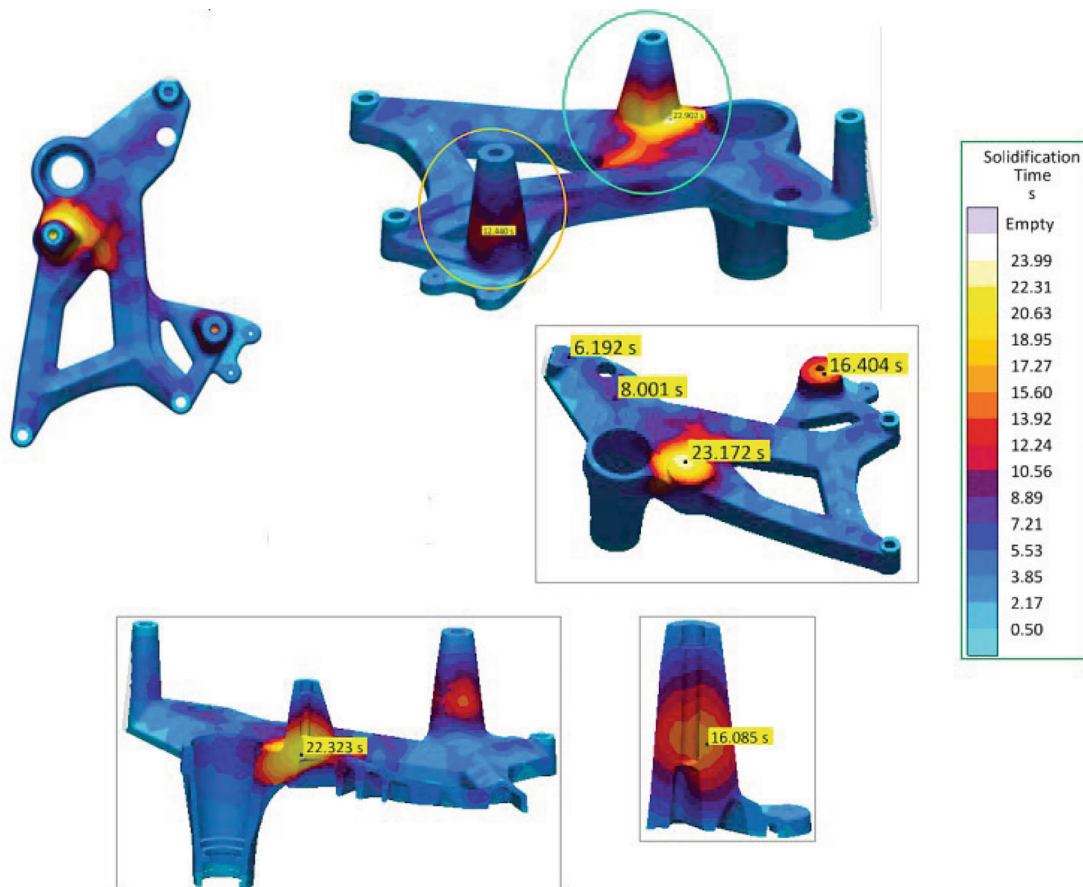


Fig. 3 Solidification time required at various regions

enhance design and minimize porosity at the proto design stage. Results indicated that thicker regions solidified last, with a maximum time of 23 s, correlating with an increased likelihood of shrinkage and porosity, as illustrated in Figs. 3, 4 and 5.

The porosity intensities in the boss regions were measured at 41, 48, 67, and 81%, as presented in Fig. 5, with

particular attention to the boss root porosity. Solidification analysis indicates a significant likelihood of porosity in the boss root areas, which contributed to the swing arm's failure during 66.6 h of durability testing. The failed component exhibited concentrated porosity near the crack, supporting previous findings that such porosity compromises material strength, resulting in structural weaknesses



Fig. 4 Hot spot shown at various regions

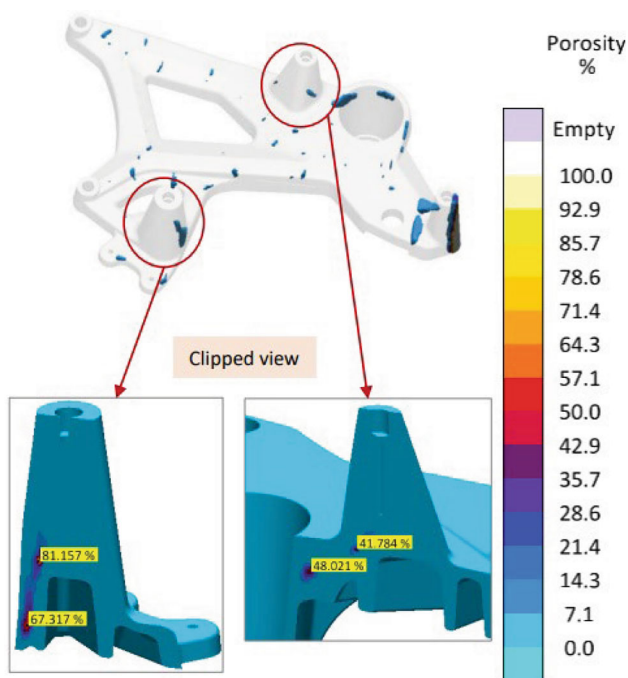


Fig. 5 Porosity intensity (%) shown at various regions

and cracks, aligning with the solidification simulation results. The solidification simulation results aligned with the porosity zones identified in the actual part. Furthermore, it was decided to take actual part porosity measurements from the same batch of manufacture.

Porosity Measurement of Failed Batch through X-ray and CT Scan A swing arm from the defective HPDC production batch was chosen for X-ray and CT scan analysis. X-ray technology measured the maximum porosity length at 4.72 mm as illustrated in Fig. 6. Subsequently, CT scan technology was utilized for porosity volumetric measurement. The CT scan results are presented in Fig. 7. The maximum pore size identified was 116.40 mm. These findings correspond with the defective part, originating from the same production batch. The porosity region was near the cracked area of the failed swing arm. A porosity length of 4.72 mm was sufficient to trigger the crack during high cycle fatigue. This phenomenon was similarly noted in a road endurance durability test lasting approximately 66.6 h. Consequently, a decision was taken to reduce the

porosity level in the HPDC aluminum swing arm to improve the component's high cycle fatigue life.

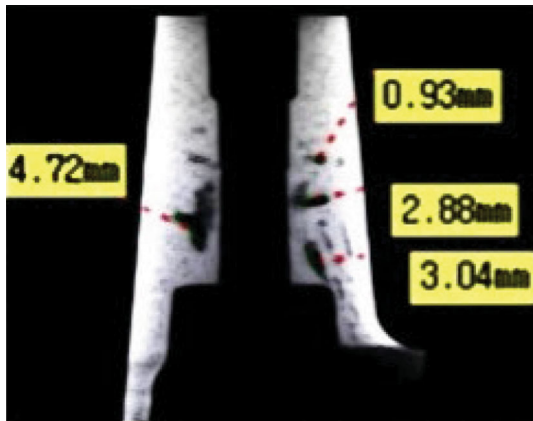
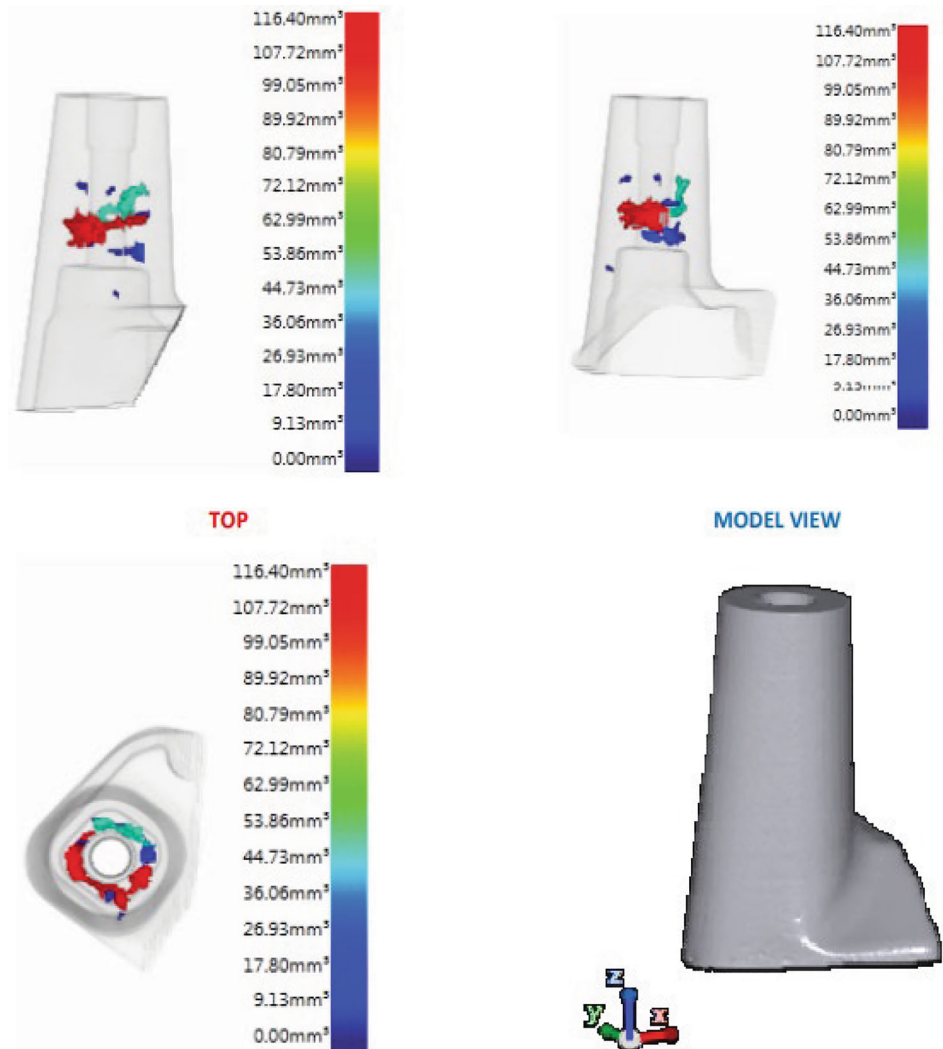
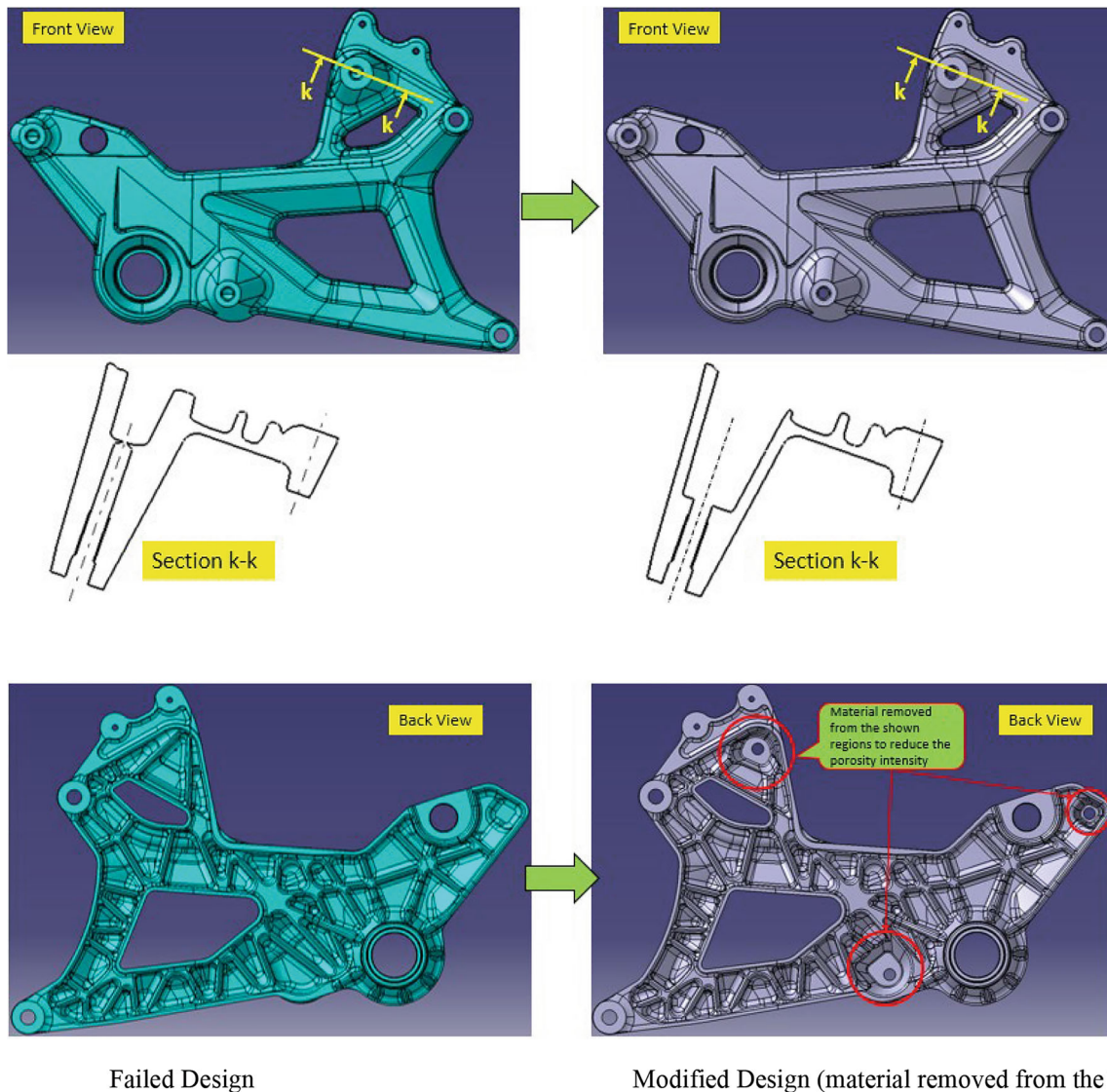


Fig. 6 X-Ray image of porosity length measurement

Fig. 7 CT scan of porosity volumetric measurement



Failure Resolution and Solidification Comparison The swing arm model was modified using Catia V5 software. Figure 8 shows a design modification involving material removal from the thicker region. This change aims to reduce solidification time and lower porosity in the swing arm. A comprehensive strength analysis precedes the evaluation of the modified design's solidification behavior. The material removal from the boss region does not affect the overall structural strength. The revised 3D model (Fig. 8) was imported into Magma 5 for solidification behavior analysis. Auto meshing was employed in the simulation as in the prior iteration. The method incorporates numerical simulation and relevant bibliographic concepts. This facilitates the interpretation of post-processing simulation data for validation through experimental testing [39, 40]. The modified design was assessed against the failed design based on specific parameters including solidification time, hot spot, and shrinkage porosity intensity as shown in Figs. 9, 10 and 11.



Failed Design

Modified Design (material removed from the bosses)

Fig. 8 Modified swing arm 3D model

Based on Chvorinov's rule mentioned below [41], efforts were made to optimize the shape of the swing arm's local section. As a result, the volume of the local geometry decreased somewhat but the surface area remained nearly unchanged.

$$ts = k \cdot M^2$$

where,

ts : The total solidification time (s);

k : solidification coefficient (s/m^2) which depends on the characteristics of the metal being cast (its density, heat capacity, and heat of fusion), the mold material (its density, thermal conductivity, and heat capacity), the mold thickness, and the amount of superheat.

M : solidification module is the ratio of the volume [V] and the surface of the (local) geometry of the casting [A] and unit is m.

As depicted in Fig. 9, solidification time was notably reduced in the modified design. The results also highlight regions with a high likelihood of casting defects. Similarly, Fig. 10 illustrates that all hotspot areas were effectively moved away from the cracked region of the failed part.

In the modified design's software simulation, as shown in Fig. 9, solidification time decreased from 16, 25, and 6 to 5, 11, and 4 s, respectively, and Fig. 10 indicates that all hotspots were relocated from the cracked region of the failed part. Overall, solidification time was minimized by at least 33%.

Longer solidification times typically lead to increased shrinkage porosity in the casting process, necessitating a

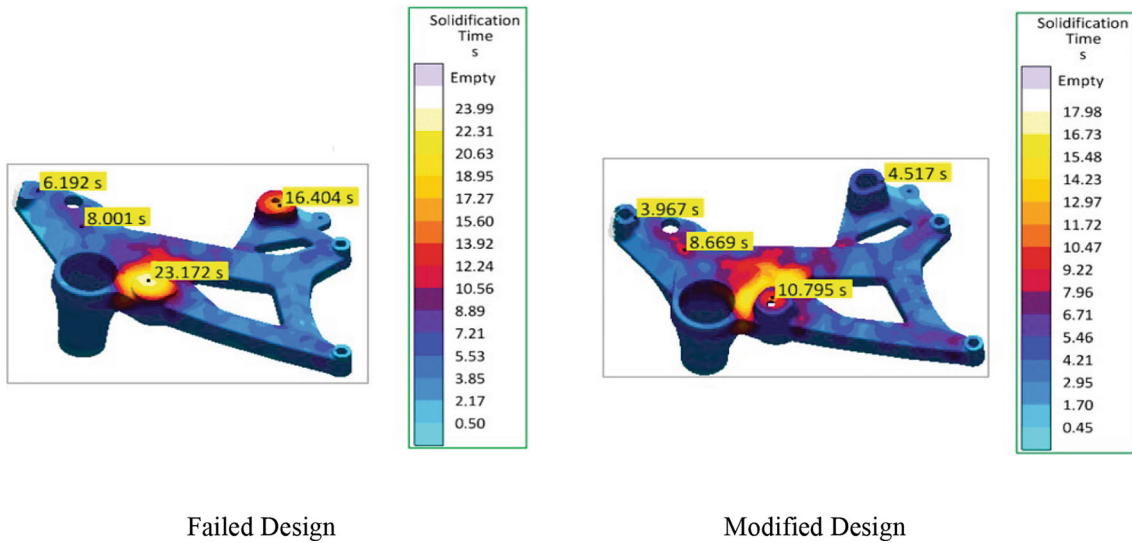


Fig. 9 Solidification time of Failed Design Vs. Modified Design

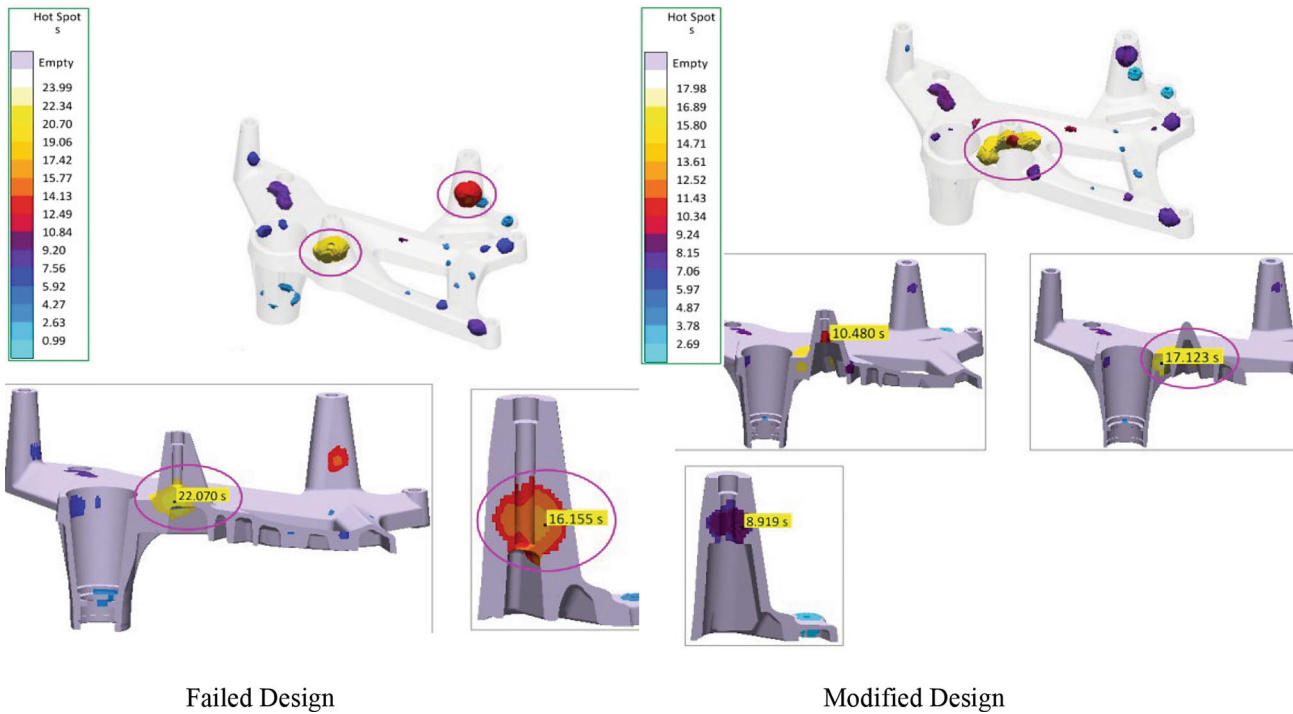


Fig. 10 Hot spot of Failed Design Vs. Modified Design

reduction in solidification time for critical areas to mitigate porosity intensity. Previous research indicates that elevated porosity levels adversely affect the fatigue life and mechanical properties of aluminum casting structures [17, 18].

As demonstrated in Fig. 11, porosity intensity in the modified design decreased from 81 to 61%, with porosity also shifting away from the cracked region of the failed part.

Modified Proto Part Development and Porosity Comparison The modified swing arm design demonstrated improved solidification behavior. Rigorous strength evaluations were conducted on the modified design using finite element analysis (FEA) simulations. The simulations included various load cases, specifically vertical loads of 3 g and lateral loads of 1 g. The observed stresses remained within acceptable limits, as shown in Fig. 12. The maximum stresses for the failed and modified designs were

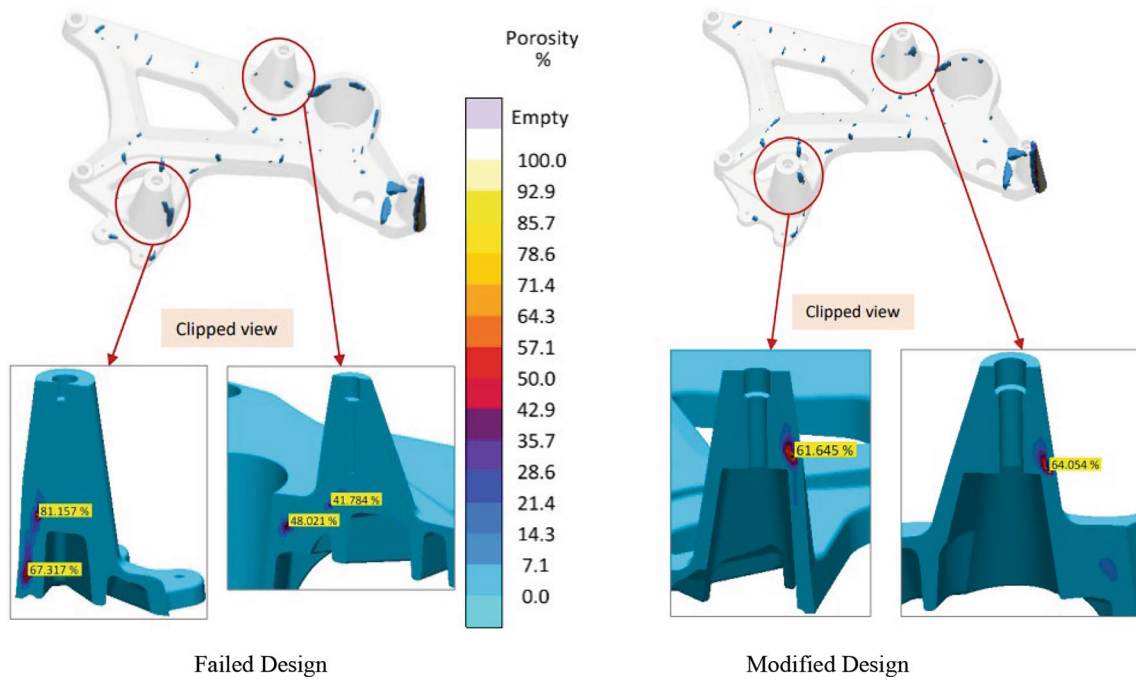


Fig. 11 Porosity intensity (%) of Failed Design Vs. Modified Design

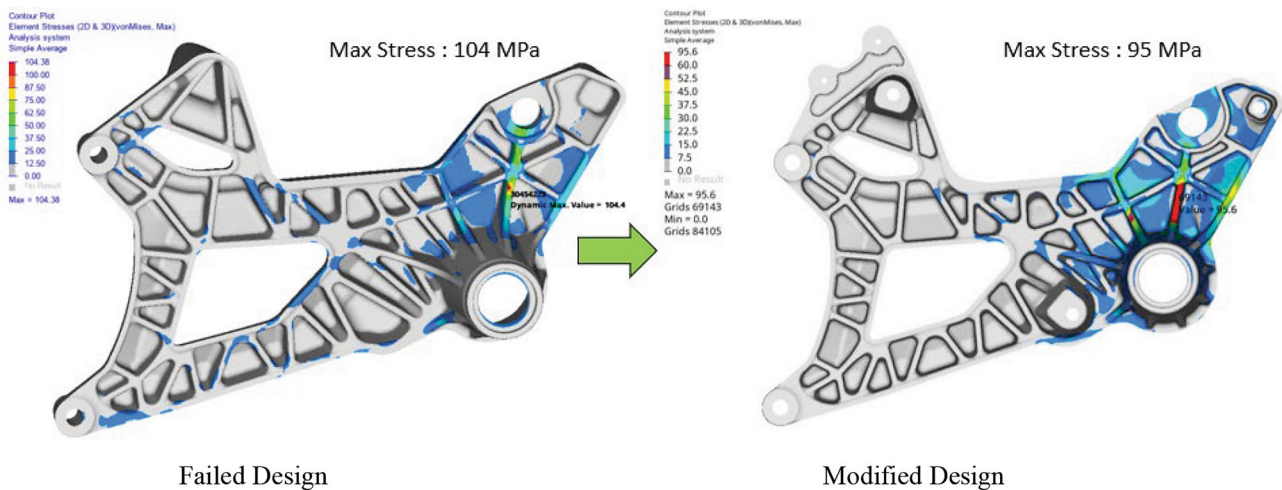


Fig. 12 Swing arm FEA analysis – 3 g vertical loading

104 and 95 MPa, respectively. Despite the removal of material to mitigate porosity in the modified design, the stress levels in the failed region did not change. The stress levels were confirmed to be acceptable, as illustrated in Fig. 13. The maximum stress recorded for the failed and modified designs was 104 and 95 MPa, respectively. In the failed region, stress levels remained constant despite modifications aimed at reducing porosity through material removal. Consequently, the decision was made to proceed with the production of prototype swing arm parts utilizing HPDC in ADC12 material.

The modified swing arm components were observed for X-ray and CT analysis. The X-ray results indicated a

decrease in pore maximum length from 4.7 to 2 mm, as illustrated in Fig. 13.

Additionally, the percentage of porosity decreased from 12.38% to 8.08%. The modified design demonstrated enhancements in both solidification simulation and actual porosity assessment. A comprehensive summary of porosity measurements is presented in Table 2.

In Table 2, % porosity represents the ratio of total pore volume in a specified area to the volume of that area within the casting structure and is estimated as below:

- (i) For failed design:

Fig. 13 X-Ray image of porosity length measurement

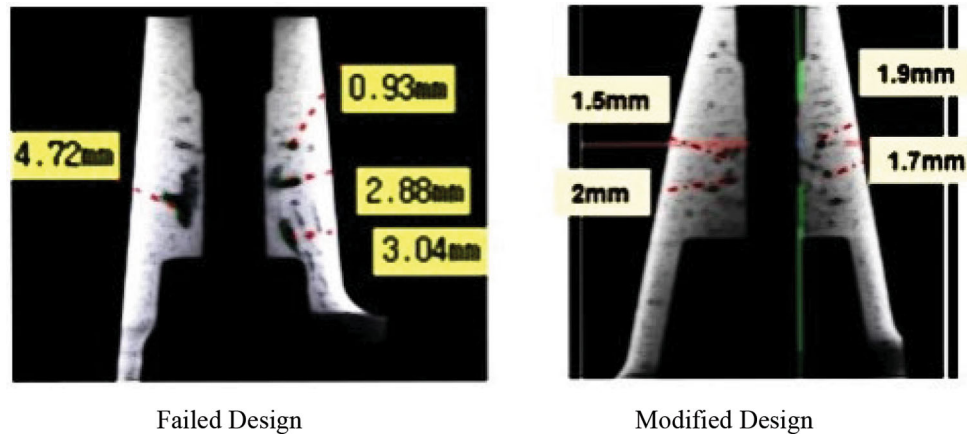


Table 2 Porosity measurement summary

Iteration	Porosity (%)	Average volume of pore (mm ³)	Max volume of pore (mm ³)	Max length of pore (mm)
Failed design	12.38	21.2	116.4	4.72
Modified design	8.08	8.27	60.05	2

Total pore volume in the local region of failed swing arm (calculated from CT scan): 6997.2 mm³.

Volume of the local region of failed swing arm (calculated from 3D data): 56520 mm³.

$$\begin{aligned} \% \text{ Porosity} &= \text{Total pore volume} / \text{3D volume of the local region (mounting boss)} \\ &= (6997.2 / 56520) \times 100 \\ &= 12.38\% \end{aligned}$$

(ii) For modified design:

Total pore volume in the local region of modified swing arm (calculated from CT scan): 3425.1 mm³.

Volume of the local region of modified swing arm (calculated from 3D data): 42390 mm³.

$$\begin{aligned} \% \text{ Porosity} &= \text{Total pore volume} / \text{3D volume of the local region (mounting boss)} \\ &= (3425.1 / 42390) \times 100 \\ &= 8.08\% \end{aligned}$$

Modified part's CT scan, depicted in Fig. 14, showed significant improvement when compared to the failed production batch. Notable reduction in maximum pore volume from 116 to 60 mm³ was observed. Porosity below 10 mm³ is negligible, as larger pores adversely affect fatigue life, based on previous research findings [1, 2, 17].

Previous studies quantitatively assessed the porosities and mechanical properties of ADC12 die castings. The

relationship between porosity and mechanical properties was analyzed, highlighting that smaller, evenly distributed pores enhance mechanical performance; porosity fractions should not exceed 3.2% for ADC12 die castings [21]. Thus, the acceptance criteria for porosity vary based on application and local criticality. In this instance, the maximum porosity acceptance criterion is set at 8.08%, with pore length limited to under 2 mm.

Testing Results The swing arm failed at 66.66 h during vehicle durability testing. Dyno testing was chosen to expedite the development process. Modified swing arm design testing was scheduled on a Dyno machine (Make: Dynostar, Model: 50 ECB) to simulate rigorous track cycles.

A comprehensive inspection using a CMM ensured the swing arm's dimensional accuracy before installation. Material test certificates were reviewed to verify compliance with specifications. The vehicle then underwent accelerated durability testing on the Dy. The test was performed under standard conditions of 24 °C and 50% humidity. Each test cycle lasted approximately 1 min. The cycle involved accelerating to 100 km/h for thirty seconds, followed by throttle release. The swing arm design was tested for 100 h (6000 cycles) on the Dyno, proving its durability and reliability. No fatigue failures were observed during the testing. Strain measurements remained within acceptable limits. Post-testing, the swing arm underwent a dye penetration test for cracks. No cracks were reported in the modified swing arm as indicated in Fig. 15.

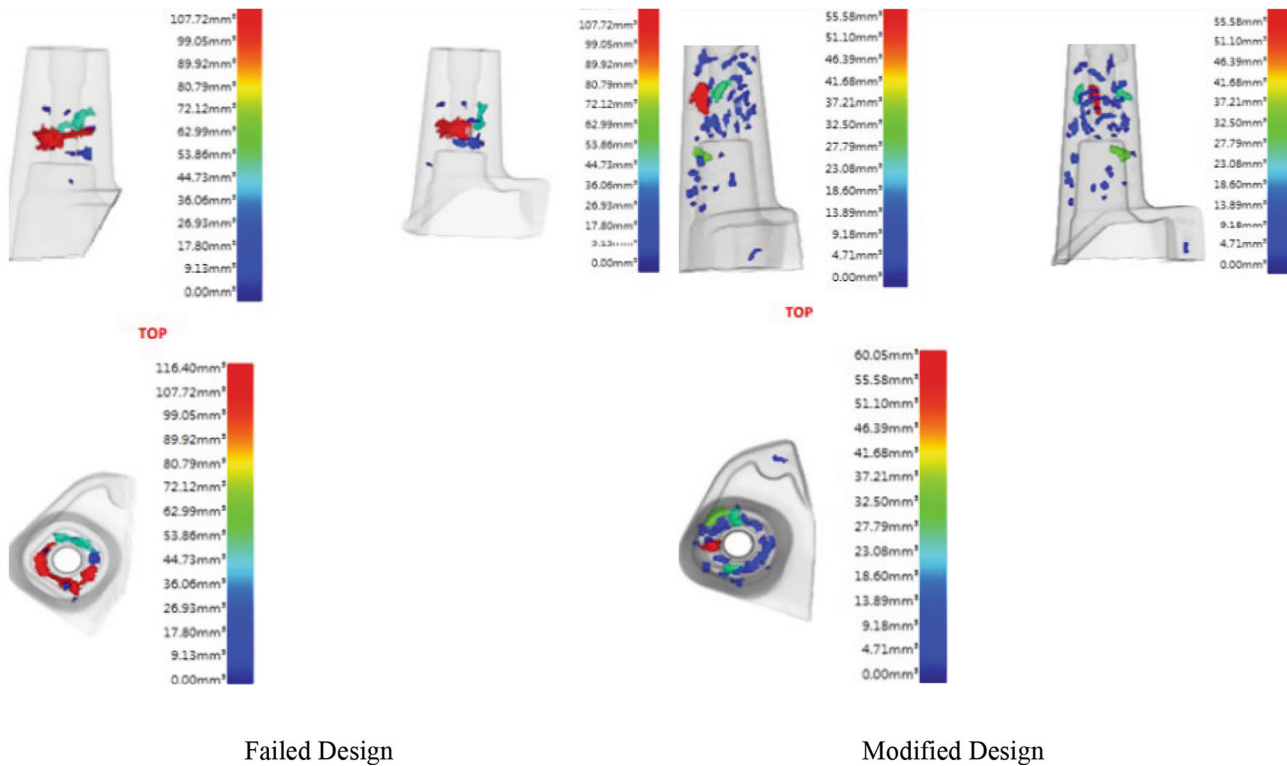


Fig. 14 CT scan of Failed Design Vs. Modified Design for porosity volumetric measurement



Fig. 15 Modified design swing arm—No crack confirmed through dye penetration

Table 3 Dyno testing summary

Iteration	Porosity (%)	Component fatigue life (h)	Increment in fatigue life (%)
Failed design	12.38	66.66	...
Modified design	8.08	100	50

Table 3 provides a summary of fatigue life findings. The modified design improves fatigue life by 50% over the failed design. During this initial vehicle development

phase, two vehicles were evaluated for both the initial and modified designs. Both vehicles with the existing design experienced failure within a similar timeframe (66–70 h). In contrast, the modified design vehicles lasted 100–110 h. The minimum values are detailed in Table 3.

Conclusions

The research study offers a comprehensive assessment of the design and development of an aluminum die-cast swing arm. The study correlates percentage porosity with component life. The focus was primarily on evaluating the solidification behavior, including pore length, solidification time, hot spot distribution, and shrinkage porosity intensity. Results indicate a notable enhancement in the fatigue life of the HPDC aluminum structure. Findings reveal that surface-remote defects have a reduced effect on fatigue strength. Conversely, pores in stressed regions significantly increase risk, while deeper defects minimally affect fatigue strength. An in-depth study was conducted on the HPDC aluminum swing arm. The removal of the material in the thicker regions lowers solidification time without affecting the strength. The reduction in solidification time results in reduction in shrinkage porosity in the casting process and thus mitigate porosity intensity. The revised design demonstrates a 50% improvement in fatigue life and a 33%

decrease in porosity. The failed design exhibited approximately 8% porosity, resulting in a fleet vehicle testing duration of 66–70 h, equivalent to 12,000 km of real-world usage. The modified design had approximately 12% porosity, achieving 100–110 h of dyno testing, corresponding to 18,000 km of actual road usage.

In conclusion, components with 8% porosity demonstrate a fatigue life equivalent to 12,000 km, while those with 12% porosity equate to 18,000 km of usage. Thus, porosity is inversely related to the fatigue life of the casting structure.

Acknowledgments Not applicable.

Funding This work did not receive any funding.

Conflict of interest The authors declare that they have no known competing financial interests or personal relationships that could have appeared to influence the work reported in this paper.

References

- V.S. Zolotarevsky et al., *Casting aluminum alloys*, 1st edn. (Elsevier Science, Amsterdam, 2007)
- Y. Li et al., Analysis of a diesel engine cylinder head failure caused by casting porosity defects. *Eng. Fail. Anal.* **127**, 105498 (2021). <https://doi.org/10.1016/j.engfailanal.2021.105498>
- M. Tebaldini et al., Estimation of fatigue limit of a A356–T6 automotive wheel in presence of defects. *Proc. Struct. Integrity.* **7**, 521–529 (2017). <https://doi.org/10.1016/j.prostr.2017.11.121>
- N. Zhang et al., Parameter optimization of Al-5Mg-3Zn-1Cu basin-shaped centrifugal casting: simulation and experimental verification. *Int. J. Metalcast.* **17**(2), 900–09 (2023). <https://doi.org/10.1007/s40962-022-00822-9>
- J. Bi et al. Process optimization of A356 aluminum alloy wheel hub fabricated by low-pressure die casting with simulation and experimental coupling methods. SSRN, (2023). <https://doi.org/10.2139/ssrn.4365913>.
- M. Jolly, L. Katgerman, Modelling of defects in aluminium cast products. *Progr. Mater. Sci.* **123**, 100824 (2022). <https://doi.org/10.1016/j.pmatsci.2021.100824>
- S. Chakravarti, S. Sen, An investigation on the solidification and porosity prediction in aluminium casting process. *J. Eng. Appl. Sci.* **70**(1), 21 (2021). <https://doi.org/10.1186/s44147-023-00190-z>
- W. Dou et al., Fatigue characterization on a cast aluminum beam of a high-speed train through numerical simulation and experiments. *Chin. J. Mech. Eng.* (2021). <https://doi.org/10.1186/s10033-021-00628-6>
- C. Lei et al., Magma software simulation assisted optimization of the casting system of turbocharger castings. *Proc. Manufact.* **37**, 59–65 (2019). <https://doi.org/10.1016/j.promfg.2019.12.013>
- H. Cao et al., Kinetic analysis of pore formation in die-cast metals and influence of absolute pressure on porosity. *Vacuum.* **168**, 108828 (2019). <https://doi.org/10.1016/j.vacuum.2019.108828>
- L. Patnaik et al., Die casting parameters and simulations for crankcase of automobile using MAGMASoft. *Mater. Today: Proc.* **22**, 563–71 (2020). <https://doi.org/10.1016/j.matpr.2019.08.208>
- R.D. Pehlke, Computer simulation of solidification processes—the evolution of a technology. *Metall. Mater. Trans. A.* **33**(8), 2251–73 (2002). <https://doi.org/10.1007/s11661-002-0349-1>
- I. Rajkumar, N. Rajini, Metal casting modeling software for small scale enterprises to improve efficacy and accuracy. *Mater. Today: Proc.* **46**, 7866–70 (2021). <https://doi.org/10.1016/j.matpr.2021.02.542>
- J.-F. Jiang et al., Numerical simulation of squeeze casting of aluminum alloy flywheel housing with large wall thickness difference and complex shape. *Trans. Nonferr. Metals Soc. China.* **33**(5), 1345–60 (2023). [https://doi.org/10.1016/S1003-6326\(23\)66187-4](https://doi.org/10.1016/S1003-6326(23)66187-4)
- Y. Li et al., Casting defects and microstructure distribution characteristics of aluminum alloy cylinder head with complex structure. *Mater. Today Commun.* **27**, 102416 (2021). <https://doi.org/10.1016/j.mtcomm.2021.102416>
- M. Wicke et al., Characterization of casting pores in Fe-Rich Al-Si-Cu alloys by microtomography and finite element analysis. *Proc. Struct. Integrity.* **2**, 2643–49 (2016). <https://doi.org/10.1016/j.prostr.2016.06.330>
- X.Y. Jiao et al., Fracture behavior of a high pressure die casting AlSi10MnMg alloy with varied porosity levels. *J. Mater. Res. Technol.* **25**, 1129–40 (2023). <https://doi.org/10.1016/j.jmrt.2023.05.281>
- P. Mu et al., Influence of casting defects on the fatigue behavior of cast aluminum AS7G06-T6. *Int. J. Fatigue.* **63**, 97–109 (2014). <https://doi.org/10.1016/j.ijfatigue.2014.01.011>
- X. Jiao et al., On the characterization of microstructure and fracture in a high-pressure die-casting Al-10 wt.%Si alloy. *Progr. Nat. Sci.: Mater. Int.* **30**(2), 221–28 (2020). <https://doi.org/10.1016/j.pnsc.2019.04.008>
- J. Wang et al., Crack configuration feature and fracture surface difference for high pressure die casting hypereutectic Al-Si alloys in high cycle fatigue. *Int. J. Fatigue.* **153**, 106469 (2021). <https://doi.org/10.1016/j.ijfatigue.2021.106469>
- H.D. Zhao et al., Experimental and numerical analysis of gas entrapment defects in plate ADC12 die castings. *J. Mater. Process. Technol.* **209**(9), 4537–42 (2009). <https://doi.org/10.1016/j.jmatprotec.2008.10.028>
- B. Yang et al., Tension-compression mechanical behavior and corresponding microstructure evolution of cast A356–T6 aluminum alloy. *Mater. Sci. Eng.: A.* **821**, 141613 (2021). <https://doi.org/10.1016/j.msea.2021.141613>
- W. Du et al., A novel method for structure's fatigue life scatter simulation under material variability. *Int. J. Fatigue.* **149**, 106296 (2021). <https://doi.org/10.1016/j.ijfatigue.2021.106296>
- Y.-C. Duan et al., Numerical prediction of fatigue life of an A356–T6 alloy wheel considering the influence of casting defect and mean stress. *Eng. Fail. Anal.* **118**, 104903 (2020). <https://doi.org/10.1016/j.engfailanal.2020.104903>
- P. Osmond et al., Effect of porosity on the fatigue strength of cast aluminium alloys: from the specimen to the structure. *Proc. Eng.* **213**, 630–43 (2018). <https://doi.org/10.1016/j.proeng.2018.02.059>
- U.A. Dabade, R.C. Bhedasgaonkar, Casting defect analysis using design of experiments (DoE) and computer aided casting simulation technique. *Proc. CIRP.* **7**, 616–21 (2013). <https://doi.org/10.1016/j.procir.2013.06.042>
- M. Avale, Casting defects and fatigue strength of a die cast aluminium alloy: a comparison between standard specimens and production components. *Int. J. Fatigue.* **24**(1), 1–9 (2002). [https://doi.org/10.1016/S0142-1123\(01\)00112-8](https://doi.org/10.1016/S0142-1123(01)00112-8)
- M.V. Santosh et al., Mechanical characterization and microstructure analysis of Al C355.0 by sand casting, die casting and centrifugal casting techniques. *Mater. Today: Proc.* **4**(10), 10987–93 (2017). <https://doi.org/10.1016/j.matpr.2017.08.056>

- 29 D.M. Maijer et al., An investigation of predictive control for aluminum wheel casting via a virtual process model. *J. Mater. Process. Technol.* **209**(4), 1965–79 (2009). <https://doi.org/10.1016/j.jmatprotec.2008.04.057>
- 30 B. Dybowski et al., Effects of die-casting defects on the blister formation in high-pressure die-casting aluminum structural components. *Eng. Fail. Anal.* **150**, 107223 (2023). <https://doi.org/10.1016/j.engfailanal.2023.107223>
- 31 S.A. Hassasi et al., Parametric investigation of squeeze casting process on the microstructure characteristics and mechanical properties of A390 aluminum alloy. *Int. J. Metalcasting.* **14**(1), 69–83 (2020). <https://doi.org/10.1007/s40962-019-00325-0>
- 32 Ö. Boydak et al., A numerical and an experimental investigation of a high-pressure die-casting aluminum alloy. *Int. J. Metalcasting.* **10**(1), 56–69 (2016). <https://doi.org/10.1007/s40962-015-0004-4>
- 33 D. Sui et al., Effect of cooling process on porosity in the aluminum alloy automotive wheel during low-pressure die casting. *Int. J. Metalcasting.* **10**(1), 32–42 (2016). <https://doi.org/10.1007/s40962-015-0008-0>
- 34 B. Yalçın et al., Effect of injection parameters and vacuum on the strength and porosity amount of die-casted A380 alloy. *Int. J. Metalcasting.* **11**(2), 195–206 (2017). <https://doi.org/10.1007/s40962-016-0046-2>
- 35 M.Y. Hu et al., Flow modeling in high-pressure die-casting processes using SPH model. *Int. J. Metalcasting.* **12**(1), 97–105 (2018). <https://doi.org/10.1007/s40962-017-0144-9>
- 36 T. Vossel et al., Influence of die temperature control on solidification and the casting process. *Int. J. Metalcasting.* **14**(4), 907–25 (2020). <https://doi.org/10.1007/s40962-019-00391-4>
- 37 D. Cica, D. Kramar, Intelligent process modeling and optimization of porosity formation in high-pressure die casting. *Int. J. Metalcasting.* **12**(4), 814–24 (2018). <https://doi.org/10.1007/s40962-018-0213-8>
- 38 W. Kasprzak et al., The effect of the melt temperature and the cooling rate on the microstructure of the Al-20% Si alloy used for monolithic engine blocks. *Int. J. Metalcasting.* **3**(3), 55–71 (2009). <https://doi.org/10.1007/BF03355453>
- 39 D. Concer, V. Marcondes, Experimental and numerical simulation study of porosity on high-pressure aluminum die casting process. *J. Braz. Soc. Mech. Sci. Eng.* **39**(8), 3079–88 (2017). <https://doi.org/10.1007/s40430-016-0672-x>
- 40 J. Jakumeit et al., Simulation-based prediction of micro-shrinkage porosity in aluminum casting: fully-coupled numerical calculation vs. criteria functions. *IOP Conf. Ser.: Mater. Sci. Eng.* **27**, 012066 (2012). <https://doi.org/10.1088/1757-899X/27/1/012066>
- 41 G. Leranth, Solidification Time estimation and simulation - in case of HPDC. *Mater. Sci. Forum.* **649**, 467–72 (2010). <https://doi.org/10.4028/www.scientific.net/MSF.649.467>

Publisher's Note Springer Nature remains neutral with regard to jurisdictional claims in published maps and institutional affiliations.

Springer Nature or its licensor (e.g. a society or other partner) holds exclusive rights to this article under a publishing agreement with the author(s) or other rightsholder(s); author self-archiving of the accepted manuscript version of this article is solely governed by the terms of such publishing agreement and applicable law.